10-2019

Mechanisms of Virus Mitigation and Suitability of Bacteriophages as Surrogates in Drinking Water Treatment by Iron Electrocoagulation

Joe Heffron
Marquette University

Brad McDermid
Marquette University

Emily Maher
Marquette University

Patrick J. McNamara
Marquette University, patrick.mcnamara@marquette.edu

Brooke K. Mayer
Marquette University, Brooke.Mayer@marquette.edu

Mechanisms of Virus Mitigation and Suitability of Bacteriophages as Surrogates in Drinking Water Treatment by Iron Electrocoagulation

Joe Heffron
Department of Civil, Construction and Environmental Engineering, Marquette University, Milwaukee, WI
Brad McDermid
Department of Civil, Construction and Environmental Engineering, Marquette University, Milwaukee, WI
Emily Maher
Department of Civil, Construction and Environmental Engineering, Marquette University, Milwaukee, WI
Patrick J. McNamara
Department of Civil, Construction and Environmental Engineering, Marquette University, Milwaukee, WI
Brooke K. Mayer
Department of Civil, Construction and Environmental Engineering, Marquette University, Milwaukee, WI

Abstract

Emerging water treatment technologies using ferrous and zero-valent iron show promising virus mitigation by both inactivation and adsorption. In this study, iron electrocoagulation was investigated for virus mitigation in drinking water via bench-scale batch experiments. Relative contributions of physical removal and inactivation, as determined by recovery via pH 9.5 beef broth elution, were investigated for three mammalian viruses (adenovirus, echovirus, and feline calicivirus) and four bacteriophage surrogates (fr, MS2, P22, and ΦX174). Though no one bacteriophage exactly represented mitigation of the mammalian viruses in all water matrices, bacteriophage ΦX174 was the only surrogate that showed overall removal comparable to that of the mammalian viruses. Bacteriophages fr, MS2, and P22 were all more susceptible to inactivation than the three mammalian viruses, raising concerns about the suitability of these common surrogates as indicators of virus mitigation. To determine why some bacteriophages were particularly susceptible to inactivation, mechanisms of bacteriophage mitigation due to electrocoagulation were investigated. Physical removal was primarily due to inclusion in flocs, while inactivation was primarily due to ferrous iron oxidation. Greater electrostatic attraction, virus aggregation, and capsid durability were proposed as reasons for virus susceptibility to ferrous-based inactivation. Results suggest that overall treatment claims based on bacteriophage mitigation for any iron-based technology should be critically considered due to higher susceptibility of bacteriophages to inactivation via ferrous oxidation.

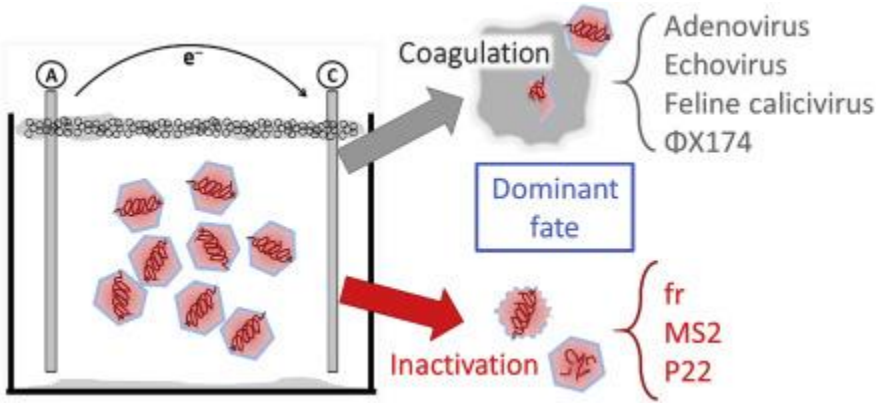

Keywords

Adenovirus, Coagulation, Disinfection, Echovirus, Feline calicivirus, Ferrous iron

1. Introduction

From 1993 to 2012, viruses were responsible for at least 24 US drinking water outbreaks reported to the Centers for Disease Control and Prevention (CDC), or 9% of all reported drinking water outbreaks in the US (Centers for Disease Control and Prevention, 2015). Viruses may be responsible for many more outbreaks that are unreported or of unknown etiology (Xagoraraki et al., 2014). Most waterborne viruses follow a fecal-oral route of infection, meaning sewage-impaired waters are a primary cause of infection (Xagoraraki et al., 2014). Worldwide, 1.8 billion people rely on sewage-contaminated drinking water (Gall et al., 2015). Viruses are persistent in the environment and resistant to many water treatment disinfection processes (Centers for Disease Control and Prevention, 2012). In addition, virus' small size makes them difficult to remove by particle separation (Tanneru and Chellam, 2013).

Among the viruses identified on the US Environmental Protection Agency's Contaminant Candidate List (CCL4) are caliciviruses (including norovirus), adenoviruses, and enteroviruses (including echovirus) (US Environmental Protection Agency, 2016). Norovirus is the leading cause of infectious diarrhea worldwide, causing as many as half of all gastroenteritis outbreaks (Grabow, 2007; Hall, 2012). Norovirus is characterized by high contagiousness, effective transmission, and rapid evolution (Hall, 2012). Due to difficulty in culturing human norovirus, surrogates such as feline calicivirus or murine norovirus are often used in laboratory tests (Bae and Schwab, 2008; Cannon et al., 2006). Adenoviruses can cause gastroenteritis in humans, as well as conjunctivitis and respiratory disease (World Health Organization, 1996). Adenoviruses are persistent in the environment and resistant to adverse conditions, as well as ultraviolet (UV) irradiation (Grabow, 2007). Echoviruses are common pathogens in human-impacted water systems. Echoviruses cause a range of diseases in humans, including gastroenteritis, meningitis, fever, and respiratory disease (World Health Organization, 1996). With diameters typically less than 30 nm, echoviruses are also among the smallest viruses (Grabow, 2007). Therefore, norovirus, adenovirus, and echovirus provide a representative suite of viruses for evaluating treatment process efficacy, due to relevance (*e.g.*, CCL4), resistance to inactivation, and resistance to physical separation.

Electrocoagulation (EC) is a promising technology for small-scale water treatment systems due to its portability and potential for automation. EC is the *in situ* production of coagulant by passing electrical current through a zero-valent sacrificial electrode, typically consisting of iron or aluminum. Portability and potential for automation make EC a good candidate for small-scale water treatment in rural or emergency applications. Small-scale treatment systems are an important market, as more than half of the public water systems in the US serve fewer than 500 people (EDR Group, 2013). Recently, EC has been considered for mitigating viruses in drinking water (Heffron et al., 2019b; Heffron and Mayer, 2016; Tanneru and Chellam, 2013, 2012; Zhu et al., 2005a). EC has shown promising results in treating bacteriophage MS2, surpassing the Surface Water Treatment Rule of 4-log virus reduction and outperforming conventional chemical coagulation for MS2 mitigation in some water matrices (Tanneru and Chellam, 2013; Zhu et al., 2005b).

In iron EC, iron is released in solution as ferrous ions (Fe^{2+}) (Lakshmanan and Clifford, 2009; Li et al., 2012). Oxidation of ferrous iron during EC can inactivate *E. coli* (Delaire et al., 2015), and steel electrodes have demonstrated higher effectiveness than aluminum or graphite electrodes for mitigating *E. coli* (Ndjomgoue-Yossa et al., 2015). Ferrous iron oxidation also inactivates bacteriophages (Jeong et al., 2006; Kim et al., 2011). Inactivation may be preferable to physical removal because active viruses removed via coagulation-flocculation could create a disposal hazard for the settled solids. In addition, promoting inactivation as well as physical removal via EC may lead to greater overall virus mitigation. However, the relative contributions of ferrous iron inactivation and physical removal have not been determined for virus inactivation during iron EC.

Bacteriophages are used as surrogates for human viruses in water treatment process research (Amarasiri et al., 2017; Grabow, 2001; Heffron and Mayer, 2016). Compared to human viruses, bacteriophage surrogates have simpler quantification and propagation protocols, propagate rapidly, and are safer to handle. To the authors' knowledge, bacteriophage MS2 has been the only virus investigated for EC or ferrous iron inactivation (Kim et al., 2011; Tanneru et al., 2014; Tanneru and Chellam, 2013, 2012; Zhu et al., 2005a). MS2 is small (approximately 25 nm diameter) and negatively charged at neutral pH (Mayer et al., 2015). Therefore, MS2 is a representative surrogate for physical treatment processes because its small, charged capsid is difficult to destabilize by charge neutralization or remove by size exclusion. However, the suitability of any surrogate must be investigated for each novel application. In the case of EC, MS2's negative charge and small size may make the bacteriophage more susceptible to transport to the anode surface and/or electrostatic attraction to a ferrous disinfectant in comparison to human viruses.

The goal of this research was to determine the fate of viruses during EC, as well as the suitability of bacteriophage surrogates to indicate enteric virus mitigation in drinking water due to EC. Fate of viruses was

distinguished as physical removal or apparent inactivation by comparing physical removal of flocs by microfiltration and elution of the bulk solution for recovery of infectious viruses. The effect of pH and other water parameters on virus mitigation was also investigated to assess the suitability of bacteriophage surrogates in a range of water matrices. To determine the mechanisms of bacteriophage mitigation, log reduction of bacteriophages due to EC was compared to chemical coagulation with ferrous and ferric chloride, sorption on floc surfaces, and electrooxidation with insoluble titanium electrodes.

2. Materials and methods

2.1. Electrocoagulation

EC tests were conducted in a 500-mL glass beaker with two plate electrodes (60 cm^2 submerged area, 1 cm inter-electrode distance) consisting of iron (mild steel), as described by Maher et al. (2019). Constant current (100 mA) was supplied by a Sorensen XEL 60–1.5 variable DC power supply (AMETEK, San Diego, CA) over a retention time of 5 min. This current and retention time were selected to achieve measurable log reduction of viruses in a range of water matrices. Current polarity was alternated at regular intervals (30 s) to maintain even electrode wear and prevent passivation (Maher et al., 2019). The reactor was stirred with a magnetic stir bar at a rate of 60 rpm ($\bar{G}$ of approximately 25 s^{-1}, although the presence of the large plate electrodes precludes accurate calculation). This stir rate was sufficient to maintain circulation between the electrodes and achieved greater bacteriophage mitigation than more rapid stirring (120 rpm) (Heffron, 2019). The electrodes and polarity-alternating controller were kindly provided by A.O. Smith Corporation. Electrodes were polished with 400 Si–C sandpaper, washed with ultrapure water and sterilized with UV light 30 min on each side in a biological safety cabinet before each test. All tests were performed in triplicate and compared to a control reactor not receiving treatment.

All tests were performed in synthetic water matrices by adding constituents to PureLab ultrapure water (ELGA LabWater, UK). Sodium nitrate (3.3 mM) was chosen as a monovalent background electrolyte, because multivalent ions can form complexes with protein moieties and thus impact surface charge (Chen and Soucie, 1986; Michen and Graule, 2010). Nitrate was chosen over chloride to avoid inactivation due to free chlorine, because chloride ions can be oxidized to form free chlorine during EC (Tanneru et al., 2014). Sodium bicarbonate was also added to achieve alkalinity typical of soft to moderately alkaline water (50 mg/L as $CaCO_3$) and prevent dramatic pH fluctuations not representative of natural water matrices (Mechenich and Andrews, 2004).

Total and ferrous iron generation due to EC was measured using Hach FerroVer Total Iron and Ferrous Iron Reagent (Hach, Loveland, CO), respectively. After EC, electrodes were rinsed with a small volume (<5 mL) of ultrapure water to remove adsorbed flocs. Generation of free chlorine was measured using Hach DPD Free Chlorine Reagent. After the addition of reagent, sample absorbance was measured using a Genesys 20 spectrophotometer (Thermo Fisher Scientific, Waltham, MA) at 510 nm (total and ferrous iron) and 530 nm (free chlorine).

2.2. Effect of water constituents on virus mitigation

In independent tests, pH, chloride, turbidity, and natural organic matter (NOM) were adjusted to assess their impact on virus mitigation. The water constituents and concentrations for all test waters are provided in Table 1. To determine the effect of water quality on virus mitigation, the background electrolyte solution was altered to compare to EC performance in the $NaNO_3$/$NaHCO_3$ electrolyte. The pH of the test water was adjusted using 0.5 N HNO_3 or NaOH. A Symphony benchtop multi-meter (VWR, Batavia, IL) was used to measure pH. Chloride (115 mg/L Cl^-) was added by replacing the background electrolyte ($NaNO_3$) with NaCl. To assess the impact of NOM, total organic carbon was increased by adding 15 mg/L C Suwannee River NOM (IHSS, St. Paul, MN). The total organic carbon contributed by virus stocks to the synthetic waters was approximately 6.5 mg/L C. For

turbidity tests, A2 test dust (Powder Technology Inc., Arden Hills, MN) was added to achieve approximately 50 NTU. NOM and turbidity conditions were chosen to represent challenging surface waters for drinking water treatment.

Table 1. Constituents added to ultrapure water to formulate synthetic waters.

	$NaNO_3$ (mg/L)	**$NaHCO_3$ (mg/L)**	**NaCl (mg/L)**	**Suwannee River Natural Organic Matter (mg/L TOC)**	**A2 Test Dust (NTU)**	**pH**
Baseline	283	84				7
Chemical coagulation	151	252				7
pH 6	283	84				6
pH 8	283	84				8
Chloride		84	190			7
NOM	283	84		15		7
Turbidity	283	84			50	7

2.2.1. Chemical coagulation

Chemical coagulation using ferrous chloride ($FeCl_2$) and ferric chloride ($FeCl_3$) was compared to EC to help determine the susceptibility of bacteriophages to inactivation/physical removal ($FeCl_2$) versus physical adsorption alone ($FeCl_3$). Doses of 2.3 mg Fe/L were used to approximate doses achieved by EC batch tests. Test waters were prepared to maintain similar conductivity to EC tests, while also providing more sodium bicarbonate alkalinity (150 mg/L as $CaCO_3$) to prevent pH fluctuation upon addition of coagulant salts, as shown in Table 1.

2.2.2. Pre-formed flocs

Viruses were added to pre-formed flocs created by EC to test for the importance of sorption to the surfaces of flocs. EC reactors were operated as for regular EC tests, except that viruses were only added to the solution after the reaction had completed. Viruses were retained for the same amount of time (5 min) under slow mixing (60 rpm) prior to sampling.

2.2.3. Titanium electrodes

To determine the potential for non-ferrous oxidant generation and oxidation at the electrode surface, iron electrodes were replaced with non-sacrificial, Grade 2 titanium plate electrodes (Performance Titanium, San Diego, CA) of the same dimensions (60 cm^2 submerged area, 1 cm inter-electrode distance). Titanium is oxidized in air to form a passive, inert electrode surface (Bagotsky, 2006). Titanium electrooxidation reactors were operated with the same parameters as the iron EC reactor (100 mA, 5 min, 30 s polarity reversal interval), as described in Section 2.1.

2.3. Virus propagation

Four bacteriophages were used as model viruses: MS2, fr, P22, and ΦX174. The properties of these bacteriophages are summarized in Table 2. In addition, three mammalian viruses were tested in varying water matrices: adenovirus 4 (ADV), echovirus 12 (ECV), and feline calicivirus (FCV; a surrogate for human norovirus), also summarized in Table 2. Bacteriophages were stored at 4 °C, while viruses were stored at −20 °C. Cryopreservant was not used to prevent adding oxidant demand associated with the virus stock solutions. Bacteriophages were spiked at concentrations of approximately 10^7 PFU/mL, while mammalian viruses were spiked at approximately 10^4 $TCID_{50}$/mL due to limitations in virus propagation.

Table 2. Properties of bacteriophage surrogates and mammalian viruses, adapted from Mayer et al. (2015) except where otherwise cited. Asterisks (*) indicate theoretical rather than measured isoelectric points.

Virus	ATCC No.	Baltimore Classification	Diameter (nm)	Isoelectric point
Bacteriophage				
fr	15767-B1	IV ((+)ssRNA)	19–23	8.9–9.0 *, 3.5 (Armanious et al., 2015)
MS2	15597-B1	IV ((+)ssRNA)	24–27	3.1–3.9 (Michen and Graule, 2010)
P22	19585-B1	I (dsDNA)	52 - 60 (Shen et al., 2008)	3.4 (Fidalgo De Cortalezzi et al., 2014)
ΦX174	13706-B1	II (ssDNA)	23–27	6.0–7.0 (Michen and Graule, 2010)
Mammalian Virus				
Adenovirus 4 (ADV)	VR-1572	I (dsDNA)	70–100	5.2 *
Echovirus 12 (ECV)	VR-1563	IV ((+)ssRNA)	24–30	6.2 *
Feline calicivirus (FCV)	VR-782	IV ((+)ssRNA)	27–41 (Prasad et al., 1994)	4.6 *

Bacteriophages were propagated using the double-agar layer (DAL) method in tryptic soy agar (BD, Franklin Lakes, NJ) (Adams, 1959). Mammalian viruses were propagated in cell cultures (see Supplementary Information [SI] 1) in sterile, 175 cm^2 culture flasks until cell monolayers were reduced to approximately 10–20% confluence, then subjected to three freeze-thaw cycles (−20 °C/22 °C). All bacteriophages and mammalian viruses were purified by two cycles of polyethylene glycol (PEG) precipitation followed by a Vertrel XF (DuPont, Wilmington, DE) extraction, as described by Mayer et al. (2008).

2.4. Virus sampling and quantification

Virus samples were taken immediately after EC. Two samples were taken from each reactor, including the control (untreated) reactor. First, a filtered sample was collected using sterile, 20-mL syringes and 0.45 µm PTFE syringe filters. Some form of physical separation is required in any coagulation process; microfiltration was chosen for this study to thoroughly separate flocs without a long flocculation step. The filter was primed with 15 mL of sample before reserving 4 mL of filtrate. The reactor was then homogenized by rapid stirring (600 rpm for 15 s), and a 20-mL sample was taken for virus elution to determine the total concentration of viable viruses in the bulk solution. To dissolve flocs and increase electrostatic repulsion between coagulant and viruses, elution was performed by adding an equal volume of pH 9.5, 6% beef extract (HiMedia, West Chester, PA) to homogenize samples and vortexing for approximately 10 s. Samples containing bacteriophages were diluted in tenfold series, and ten 10-µL drops of each dilution were plated using the spot titer plaque assay method, as described by Beck et al. (2009). Mammalian viruses were quantified using the Reed & Muench $TCID_{50}$ method (Reed and Muench, 1938). Virus recovery was confirmed in numerous tests, *e.g.*, at pH 8 (Fig. 1) and in waters containing turbidity and NOM (Fig. 2). Confirmation of bacteriophage recovery by elution was demonstrated using chemical coagulation with ferric chloride (Fig. 3).

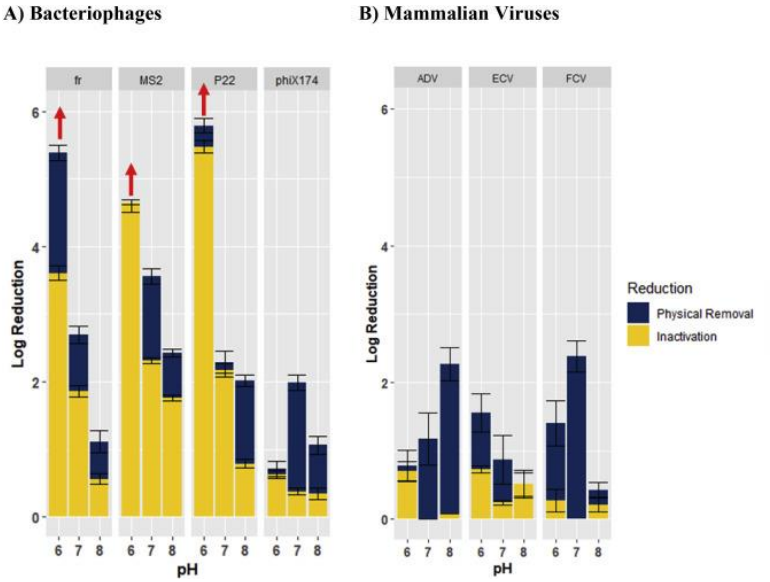

Fig. 1. Effect of pH on inactivation and physical removal of A) bacteriophages and B) mammalian viruses due to electrocoagulation. Upward arrows indicate log reduction beyond the countable limit, so values shown are the limit of quantification. Error bars represent standard error of the mean of triplicate tests.

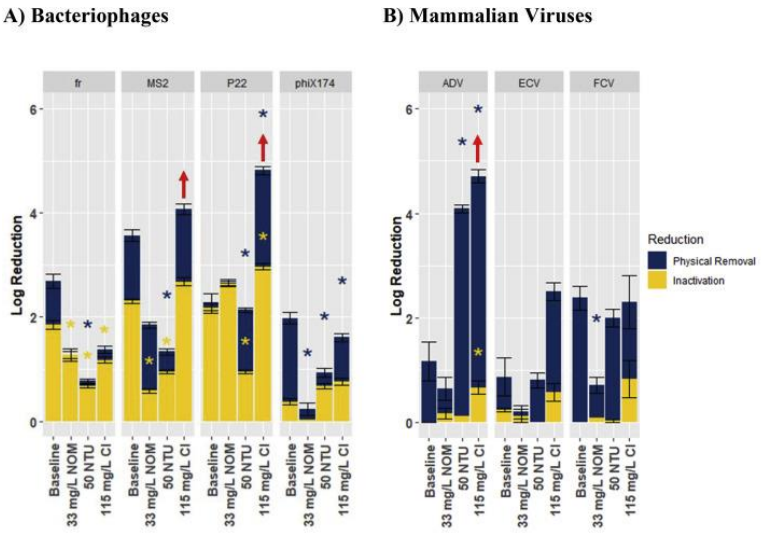

Fig. 2. Effect of water constituents on inactivation and physical removal of A) bacteriophages and B) mammalian viruses due to electrocoagulation. Asterisks indicate a significant difference in log reduction from the baseline condition (pH 7, simple electrolyte) due to physical removal (blue asterisk) or inactivation (yellow asterisk). Upward arrows indicate log reduction beyond the countable limit, so values shown are the limit of quantification. Error bars represent standard error of the mean of triplicate tests. (For interpretation of the references to color in this figure legend, the reader is referred to the Web version of this article.)

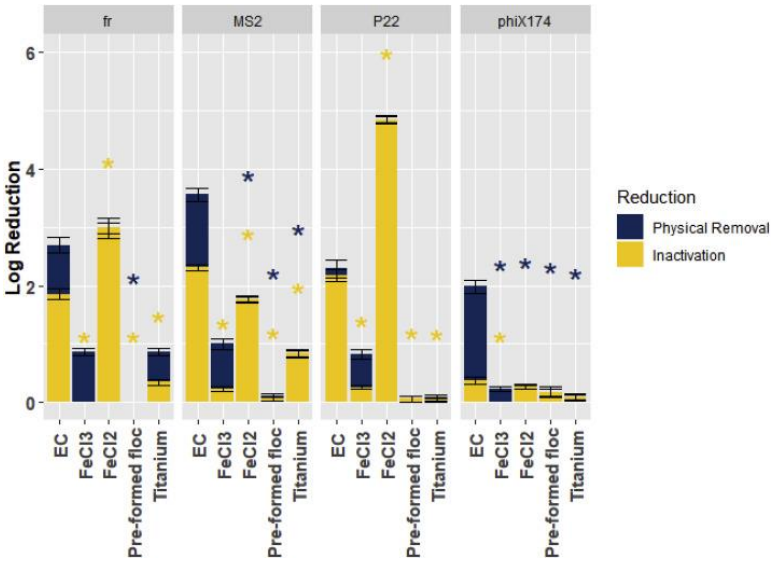

Fig. 3. Mechanisms of bacteriophage mitigation due to electrocoagulation, chemical coagulation, adsorption and electrooxidation. Inactivation and physical removal were compared between electrocoagulation (EC), chemical coagulation with ferric chloride ($FeCl_3$), chemical coagulation with ferrous chloride ($FeCl_2$), flocs formed by electrocoagulation prior to the addition of bacteriophages (pre-formed floc), and electrooxidation with inert titanium electrodes (Titanium). Asterisks indicate a significant difference in log reduction from electrocoagulation due to physical removal (blue asterisk) or inactivation (yellow asterisk). Error bars represent standard error of the mean of triplicate tests. (For interpretation of the references to color in this figure legend, the reader is referred to the Web version of this article.)

Virus mitigation (total reduction in the number of infectious viruses) was distinguished as inactivation or physical removal based on recovery of infectious viruses from the filtered and eluted samples. The log reduction in infectious viruses between the filtered control and filtered treated samples represented total mitigation (Eqn. (1)). The log reduction in infectious viruses between the eluted control and eluted treated samples represented inactivation, *i.e.*, viruses that could not be recovered from the bulk solution (including flocs, Eqn. (2)). Mitigation due to physical removal was therefore the difference between total mitigation and inactivation, *i.e.*, the fraction of total mitigation that was recoverable from the bulk solution by elution (Eqn. (3)).(1)TotalMitigation=FiltrateControl−FiltrateTreated(2)Inactivation=EluateControl−EluateTreated(3)PhysicalRemoval=TotalMitigation−Inactivation

Notably, we attributed all irrecoverable loss of infectious viruses to apparent inactivation in this study. However, recovery of viruses from solid phases such as flocs is challenging, and losses could also reflect variation in elution efficiency (as discussed further in Section 3.2.3). The elution method used in this study was previously used to determine virus inactivation due to EC and chemical coagulation (Heffron et al., 2019a; Matsui et al., 2003; Tanneru et al., 2014). Here, it showed reliable recovery of bacteriophages after coagulation with ferric chloride: fr, 98%; MS2, 59%; P22, 55%; ΦX174, 99% (Fig. 3, the “inactivated” fraction represents non-recoverable viruses for $FeCl_3$ treatment). Recovery of mammalian viruses after EC also showed reliable recovery, for example at pH 7: ADV, 100%; ECV, 58%; FCV, 100% (Fig. 1). Irrecoverable virus mitigation via EC was compared to these benchmark recoveries in order to verify inactivation, and in many cases, inactivation was multiple logs greater.

Molecular methods (*e.g.,* qPCR) can be effective in qualitatively determining inactivation by either demonstrating genome damage or in combination with cultural techniques, showing the presence of viral genomes in the absence of infectious viruses. Previous work has demonstrated bacteriophage inactivation due

to ferrous and zero-valent iron using both immunosorbent assay and qPCR (Kim et al., 2011). However, a reliable molecular method for quantifying virus inactivation is not currently available. Likewise, molecular methods cannot distinguish between aggregated and dispersed virions, so techniques like qPCR cannot be used to validate virus elution. Since nucleic acids are also susceptible to both physical adsorption and oxidative fragmentation, even time- and resource-intensive combined cultural and molecular methods still have a degree of uncertainty in quantitatively determining fate. Therefore, cultural assays showing irrecoverable mitigation with a proven method of recovery remain the most direct means of quantifying inactivation in processes that also exhibit physical removal (Heffron and Mayer, 2016).

2.5. Mechanisms of virus mitigation

To establish mechanisms of virus mitigation, log reduction due to EC was compared to similar physical/chemical processes (chemical coagulation and electrochemical oxidation). These tests were only performed with bacteriophages due to limited inactivation of mammalian viruses by EC.

2.6. Zeta potential and particle size measurement

The zeta potential of bacteriophage fr and A2 test dust were confirmed by dynamic light scattering (DLS) using a Zetasizer Nano-ZS (Malvern Panalytical, Malvern, UK), software version 7.11. Bacteriophage fr was chosen for zeta potential analysis (pH 1.0–9.3) due to wide discrepancy in isoelectric point values reported in the literature, as shown in Table 2. Bacteriophage aggregation was similarly evaluated by measuring particle size via DLS over a range of pH values (pH 6–8). For both zeta potential and particle size measurements, the buffered demand-free (BDF) solution used for bacteriophage propagation was replaced with “Baseline” electrolyte (Table 1) by dialysis. Bacteriophage stocks were transferred to Slide-A-Lyzer 20 kDa MWCO dialysis cassettes (Thermo Scientific, Waltham, MA) and stirred at 4 °C for 3 days with daily replacement of electrolyte solution. A2 test dust was diluted to 0.6 g/L in ultrapure water. The “Baseline” electrolyte was adjusted to near target pH with 0.5 M NaOH or HNO_3. Samples were added to pH-adjusted electrolyte in a 1:4 dilution for a final bacteriophage concentration of approximately 10^8–10^9 PFU/mL. Final pH was read simultaneously with zeta potential and particle size readings.

2.7. Data analysis

All statistical analyses were performed in the R statistical language using the stats package (R Core Team, 2014). Mean log reduction by physical removal and inactivation was compared between test conditions using independent, 2-tailed Student's t-tests ($\alpha = 0.05$) with a Bonferroni correction for multiple comparisons. The effect of pH on bacteriophage inactivation was evaluated by linear regression. (The mammalian viruses did not show a uniform trend of inactivation, so inactivation at pH 6, 7, and 8 was compared by t-tests.) Models were evaluated for residual distribution, normality, and leverage points using the plot. lm () function, and significance of variables was evaluated by analysis of variance with the anova () function (R Core Team, 2014). A link for all R scripts is provided in SI 2.

3. Results and discussion

3.1. Effect of water constituents on virus mitigation

The mitigation of bacteriophages and viruses via EC was evaluated over a wide range of water matrices. In order to isolate the effects of pH, NOM, turbidity, and chloride on virus mitigation by EC, artificial water matrices were prepared by varying these parameters individually. The relative importance of physical removal and inactivation via EC, here determined as recoverable vs. irrecoverable virus mitigation, respectively, was compared between bacteriophages and viruses.

3.1.1. Effect of pH

Both mammalian viruses and bacteriophages were inactivated and physically removed to some degree over the pH range tested (pH 6–8), as shown in Fig. 1. However, whereas inactivation was the dominant fate for bacteriophages fr, MS2, and P22, bacteriophage ΦX174 and mammalian viruses showed the greatest mitigation due to physical removal. The physical removal of viruses in flocs is influenced by numerous factors, including electrostatic repulsion and van der Waals attraction (modeled by the DLVO theory), and non-DLVO factors such as hydrophobicity, steric hindrance, virus aggregation, and interactions with water matrix constituents (Heffron and Mayer, 2016).

Inactivation was most pronounced at low pH. All four bacteriophages (including ΦX174) demonstrated a significant exponential relationship between log inactivation and pH, as summarized in SI 3. Similarly, inactivation was greatest at low pH (pH 6) for all mammalian viruses except FCV, which was not effectively inactivated at any pH ($p > 0.21$). (Possible reasons for differences in virus resistance to inactivation are discussed in Section 3.3.) Inactivation was significantly greater at pH 6 than pH 7 for ADV ($p = 0.0027$) and ECV ($p = 0.00025$), though only approximately 0.7 log inactivation was achieved at pH 6 for either virus. These results support previous findings (Heffron et al., 2019a; Kim et al., 2011) that MS2 and P22 inactivation in ferrous iron-based treatment processes is greater at lower pH. However, this phenomenon has only been demonstrated previously with bacteriophages. These results show that bacteriophages commonly used in water treatment testing were inactivated to a far greater degree than the mammalian viruses in this study.

Bacteriophage ΦX174 was far more resistant to inactivation than the other bacteriophages, with only 0.6 log inactivation at pH 6. Total ΦX174 mitigation was greatest at pH 7. Since the isoelectric point (pI) of ΦX174 is near neutral (Michen and Graule, 2010), ΦX174 would be more likely to destabilize and aggregate due to van der Waals interactions at pH 7, which likely contributed to greater physical removal at pH 7. In addition, aggregation can reduce the efficacy of disinfection (Gerba and Betancourt, 2017). The impact of pH on physical removal was difficult to interpret for bacteriophages fr, MS2, and P22, because differences in physical removal may have been an artifact of the decrease in total mitigation at higher pH.

As with inactivation, physical removal of the mammalian viruses was more similar to that of ΦX174 than the other bacteriophage surrogates. Total mitigation varied slightly with pH for the mammalian viruses, though no unifying trend was apparent. ECV showed a weak trend of greater physical removal at low pH. The theoretical pI of ECV is approximately 6.2 (Mayer et al., 2015), which could explain greater physical removal at pH 6. Only FCV showed a significant difference in physical removal between pH levels, with poorer removal at pH 8 than pH 7 ($p = 0.000250$). Conversely, ADV showed a weak trend of greater physical removal with increasing pH. However, the low mitigation of the mammalian viruses relative to the variance makes it difficult to make meaningful inferences between means. For the purpose of identifying a representative virus surrogate, the very fact that mammalian virus removal was consistently low (<2.5 log) is more important. Only bacteriophage ΦX174 mitigation remained below the bar of 2.5 log total mitigation over the pH range tested.

3.1.2. Effect of natural organic matter

The presence of NOM was generally inhibitory to both inactivation and physical removal, as shown in Fig. 2. Suwannee River NOM consists primarily of fulvic acid (65% by weight) with a lesser fraction of humic acid (10%) (Averett et al., 1994). The pKa of fulvic acids found in Suwannee River NOM is in the range of 2–4, indicating a negative charge at neutral pH (Leenheer et al., 1995). Therefore, NOM may inhibit physical removal and disinfection by sorbing the iron required for virus destabilization and disinfection. Once complexed with NOM, ferrous iron is resistant to oxidation by dissolved oxygen or free chlorine (Crittenden et al., 2012). Tanneru and Chellam (2012) similarly found poor mitigation of MS2 using iron EC in natural river water and synthetic waters containing humic acid. Bacteriophage P22 was not inhibited by NOM in this study, though the reasons are

unclear. We are not aware of any direct comparison of P22 hydrophobicity to that of other bacteriophages that might help explain the lesser impact of NOM. As a large virus, more of the P22 capsid may be exposed to oxidants when sorbed to NOM. Bacteriophage ΦX174 mitigation was nearly completely inhibited (<0.25 log reduction), indicating that ΦX174 continued to be an appropriate surrogate for the mammalian viruses in high-NOM water matrices.

3.1.3. Effect of turbidity

Turbidity also inhibited inactivation, though the impact of turbidity on physical removal was mixed, as shown in Fig. 2. Bacteriophages fr, MS2, and P22 all demonstrated poorer inactivation in turbid water, while ΦX174 showed minimal inactivation even without added turbidity. A2 test dust consists primarily of silica (69–77%) and alumina (8–14%), as well as various metal oxides (Powder Technology Inc., 2016). The presence of reduced metal species in sand can present a significant oxidant demand (Huling and Pivetz, 2006). Accordingly, metal oxides in A2 test dust may scavenge oxidants and therefore inhibit viral inactivation.

Turbidity also inhibited physical removal of fr, MS2, and ΦX174. A2 dust was demonstrated by DLS to have a strong negative zeta potential around neutral pH, as shown in SI 4. Therefore, the test dust likely had a coagulant demand that inhibited virus removal at low coagulant doses. Zhu et al. (2005a) found that silica increased MS2 reduction by ferric chloride coagulation–microfiltration; however, silica created a coagulant demand that impaired treatment at low coagulant doses (<5 mg/L) similar to those used in this experiment. Diverse constituents contribute to turbidity in the environment; accordingly, the effect of turbidity may vary in natural water sources.

Both bacteriophage P22 and ADV had greater removal by physical removal with increased turbidity. As the largest viruses tested (50–100 nm diameter), P22 and ADV were likely retained due to internal fouling or formation of a cake layer during filtration of the turbid samples. Using the same filtration technique as in EC experiments, filters fouled with EC flocs and turbidity significantly rejected P22 (1.27 log reduction, $p = 2.01 \times 10^{-5}$) to a greater degree than MS2 (0.66 log reduction, $p = 0.00014$), as detailed in SI 5. The greater degree of rejection for large viruses may override the coagulant demand of the A2 dust. Smaller bacteriophages like MS2, which saw a small increase in rejection by the fouled filter, may have been adversely affected to a greater degree by the decrease in available coagulant. In Zhu's study (2005a), development of a cake layer did not enhance dead-end microfiltration of the smaller MS2 bacteriophage following ferric chloride coagulation.

3.1.4. Effect of chloride

Chloride was expected to increase inactivation through the production of free chlorine at the anode (Tanneru et al., 2014). However, inactivation significantly increased only for P22 and ADV, while inactivation decreased slightly for bacteriophage fr (Fig. 2). No other viruses showed significant changes in mitigation with the addition of chloride. In the absence of viruses, the chlorine residual in the bulk solution during EC remained below the detection limit of 0.02 mg/L Cl_2. Most of the chlorine generated by chloride oxidation would likely be scavenged by ferrous iron, which is also produced at the anode surface. Tanneru et al. (2014) similarly found poor inactivation of bacteriophage MS2 due to free chlorine generation with aluminum EC. Aluminum EC would be expected to show greater efficiency in producing free chlorine than iron EC, because aluminum ions are oxidized to a stable form at the electrode and would not exert oxidant demand in solution (Cañizares et al., 2007). Further research comparing relative virus susceptibility to free chlorine and ferrous iron is needed to understand why inactivation increased for the two large viruses (bacteriophage P22 and ADV), but remained the same or slightly decreased for the remaining bacteriophages and viruses.

The rate of iron generation by EC increased dramatically in the presence of chloride, as shown in SI 6. Carbon steel is susceptible to increased corrosion rates and pitting in the presence of chloride (Song et al., 2017).

Therefore, the greater iron generation was likely due to chemical corrosion. The greater iron dose (6.6 mg/L Fe) may have impacted physical removal, increasing mitigation of P22 and ADV by physical removal but decreasing ΦX174 mitigation. Again, the largest viruses (P22 and ADV) showed increased physical removal, possibly indicating retention of viruses due to membrane fouling during filtration. In the case of ΦX174, lower removal at higher doses may seem paradoxical. However, total removal of ΦX174 was not significantly different from total removal without chloride, so the decrease in physical removal represents only a shift in mechanism of mitigation.

3.2. Mechanisms of virus mitigation

To determine why some bacteriophages demonstrated inactivation due to EC, the mechanisms of bacteriophage mitigation were investigated. Understanding the reason why some bacteriophages are inactivated by ferrous iron may help in selection of better virus surrogates or to identify more susceptible pathogen targets. As shown in Fig. 3, ferric chloride coagulation and ferrous chloride coagulation reasonably predicted whether inactivation or physical removal was the predominate bacteriophage fate in EC, whereas adsorption to preformed flocs and electrooxidation were not important mechanisms. Previous research (Heffron et al., 2019a; Kim et al., 2011; Tanneru and Chellam, 2012) has found a correlation between oxidation of ferrous iron (Fe^{II}) and bacteriophage inactivation. Therefore, chemical coagulation with $FeCl_2$ was expected to achieve inactivation, whereas the already oxidized ferric coagulant ($FeCl_3$) should achieve only physical removal.

Compared to chemical coagulation with $FeCl_3$, EC resulted in significant inactivation for all bacteriophages (*p*-values: fr, 3.69×10^{-6}; MS2, 1.33×10^{-6}; P22, 5.63×10^{-6}; and ΦX174, 1.01×10^{-3}), though ΦX174 mitigation was predominately due to physical removal. Like EC, chemical coagulation with $FeCl_2$ showed substantial inactivation of fr, MS2, and P22, but only slight inactivation of ΦX174. More importantly, chemical coagulation with $FeCl_2$ resulted in an even greater discrepancy in inactivation between ΦX174 and the other bacteriophages than was observed with EC. Inactivation of fr and P22 was greater with $FeCl_2$ than EC, though MS2 inactivation was slightly greater with EC than $FeCl_2$. Greater inactivation with $FeCl_2$ might have occurred because the entire concentration of ferrous iron was added at once and thoroughly mixed to provide a higher and more homogenous ferrous concentration throughout the reactor. Despite differences in the final log inactivation between $FeCl_2$ and EC, the effect of ferrous iron is sufficient to explain inactivation observed in EC. Conversely, chemical coagulation with $FeCl_3$ achieved only physical removal. For fr, MS2, and P22, EC achieved a similar degree of physical removal as $FeCl_3$ coagulation, and EC outperformed chemical coagulation for ΦX174.

3.2.1. Pre-formed flocs

No bacteriophages demonstrated mitigation (neither inactivation nor physical removal) when added to reactors containing flocs pre-formed by EC. Therefore, sorption to flocs was not a significant mechanism of virus mitigation in simple electrolyte solution. Instead, physical removal in EC is due to inclusion of viruses within the developing floc. Other researchers (Kreiβel et al., 2014; Shirasaki et al., 2016, 2009) have similarly found greater virus mitigation during rapid mixing and floc formation. The importance of inclusion of viruses in the floc may also explain why EC was more effective than $FeCl_3$ chemical coagulation for mitigating ΦX174. In EC, coagulant is gradually added to solution, which typically slows floc formation in comparison to chemical coagulation (Harif et al., 2012); thus EC allows longer contact time for virus inclusion within the floc.

3.2.2. Titanium electrodes

Uncoated titanium electrodes were used to evaluate the potential for bacteriophage mitigation due to generation of non-ferrous oxidants (*e.g.*, reactive oxygen species) and/or oxidation at the anode surface. Air-oxidized titanium anodes are stable in aqueous solutions, extracting electrons from species in solution rather than dissolving like iron (Bagotsky, 2006; Wilhelmsen, 1987). Titanium electrooxidation mitigated both MS2 and fr, though less than one log total reduction was achieved. No significant mitigation was found for P22 or ΦX174.

Titanium electrodes are likely to overestimate the effects of inactivation, because a) ferrous iron may scavenge oxidants, and b) oxidation of the iron electrode competes with other oxidation reactions at the electrode surface. Nevertheless, inactivation with titanium electrodes was far less than with iron electrodes. Therefore, neither anodic oxidation nor generation of non-ferrous oxidants can be considered important mechanisms of virus mitigation under the conditions investigated in this study. This finding further confirms that ferrous oxidation is the primary determinant of inactivation due to EC.

3.2.3. Inactivation or irreversible coagulation?

In this study, the irrecoverable loss of infectious bacteriophages was attributed to inactivation. The pH 9.5 beef broth elution used to recover bacteriophages and mammalian viruses is an established method for both EC and chemical coagulation (Heffron et al., 2019a; Matsui et al., 2003; Tanneru et al., 2014). Bacteriophage recovery was established using $FeCl_3$ chemical coagulation (Fig. 3), while virus recovery was demonstrated at neutral pH using EC (Fig. 1). However, the difference in virus concentration between the control and the treated eluate, here defined as inactivation, could possibly reflect differences in elution efficacy between viruses and coagulant types, and therefore fail to accurately assess inactivation across all tests.

Flocs generated by chemical coagulation tend to be more structurally robust than those formed by EC due to differing kinetic limitations (Harif et al., 2012). Therefore, elution methods successful for chemical coagulation (*i.e.*, with $FeCl_3$) should suffice for EC based on floc structure alone. Perhaps more importantly, flocs formed by EC may be composed to varying degrees of ferrous as well as ferric iron (Dubrawski et al., 2015). Since $FeCl_2$ chemical coagulation also resulted in irrecoverable bacteriophage mitigation, $FeCl_2$ could not be used to validate virus elution from flocs. However, Heffron et al. (2019a) used the same elution method to demonstrate that irrecoverable bacteriophage mitigation was proportional to ferrous iron oxidation, and that bacteriophages exposed to ferrous iron could not be recovered even after complete oxidation to ferric iron. Since the irrecoverable loss of bacteriophages increased as the iron oxidized to the ferric form (for which the elution method was proven effective), the irrecoverable fraction must be due to oxidative inactivation. In addition, the excellent recovery of human viruses in this study indicates that this elution method is appropriate for EC as well as conventional coagulation. For these reasons, the irrecoverable fraction was attributed to apparent inactivation. While losses may include inactivation as well as irreversible coagulation, this does not impact the primary finding of this study regarding inactivation: that fr, MS2, and P22 bacteriophages are too susceptible to EC and ferrous iron to serve as reliable indicators of virus mitigation.

3.3. Virion properties and ferrous susceptibility

3.3.1. Isoelectric point

Of the mechanisms of bacteriophage mitigation discussed in Section 3.2, susceptibility to ferrous inactivation was the primary cause of differences in log reduction between bacteriophages fr, MS2, and P22 on the one hand, and bacteriophage ΦX174 and the mammalian viruses on the other. Ferrous cations differ from neutrally- or negatively-charged disinfectants such as free chlorine. Though the positive ferrous charge may enhance disinfection of negatively-charged pathogens, pathogens with a positive charge near neutral pH may be repelled.

In addition, aggregation can shield viruses and reduce the efficacy of disinfection (Gerba and Betancourt, 2017). Since iron-based inactivation is more effective at lower pH (Kim et al., 2011), viruses with pIs near pH 6–7 would therefore tend to aggregate due to charge neutralization and become shielded under the conditions of greatest disinfection capacity in this study. Bacteriophage ΦX174 showed marked aggregation near pH 7 based on measurement of particle size by DLS, as shown in SI 7. Other bacteriophages did not demonstrate similar aggregation at circumneutral pH. Thus, electrostatic repulsion and aggregation may explain the poor inactivation of ΦX174 (pI = 6.0–7.0) compared to bacteriophages fr, MS2, and P22, which have low pIs (<4, see Table 2). Because pI values reported in the literature varied widely for bacteriophage fr (pI = 3.5 to 9.0), the pI for fr was

experimentally validated in this study at approximately 2.7, as shown in SI 4. Enteric viruses often enter the water cycle as aggregates (Gerba and Betancourt, 2017), and much of the viral load for drinking water treatment is associated with particles (Springthorpe and Sattar, 2007). Therefore, the tendency of viruses to aggregate is similarly an important factor for EC treatment of natural waters.

Bacteriophage ΦX174 may also have been mitigated to a lesser extent than other bacteriophage surrogates due to structural robustness. Whereas F-specific bacteriophages like fr and MS2, as well as tailed bacteriophages like P22, have a single locus of attachment and penetration, ΦX174 can attach to and penetrate host cells at any of 12 spikes occurring at the capsid's 5-fold vertices (Sun et al., 2013). However, ΦX174 has not been shown to have similarly high resistance to other disinfectants, and the single maturation protein of F-specific bacteriophages does not appear to be an Achilles heel for chemical disinfection (Heffron and Mayer, 2016). Therefore, there is little evidence to support the theory that ΦX174 is inherently more robust than other bacteriophages.

While experimental values are not available for ADV and ECV isoelectric points, both viruses are resistant to inactivation and have theoretical isoelectric points close to neutral (5.2 and 6.2, respectively, see Table 2). However, FCV is one possible exception to the hypothesis that electrostatic forces determine ferrous disinfection. FCV has a theoretical pI of 4.6, and virus-like particles consisting of FCV capsid proteins have a similar reported pI of 3.9 (Samandoulgou et al., 2015). Therefore, the FCV capsid likely has a negative charge at neutral pH and should attract ferrous ions, yet FCV remains resistant to ferrous-based inactivation. Therefore, isoelectric point may be insufficient to fully explain ferrous susceptibility.

3.3.2. Capsid structure

A review of capsid structure provides some insight into the resistance of mammalian viruses. Protein structures for bacteriophages and viruses were accessed from the VIPERdb database (TSRI, 2018), as summarized in Table 3. Structural files for adenovirus 4 were not available, so adenovirus serotypes 5 and 26 were used instead. (Both ADV5 and ADV26 shared similar dimensions, despite representing different species.) Crenulations and protuberances on the capsid surface can result in outer diameter values not representative of actual capsid thickness, and the method of structural analysis influences the degree of detail captured on the capsid surface (Pettigrew et al., 2006). To minimize the influence of surface features, “adjusted” capsid thickness was obtained by subtracting the inside diameter from the average diameter (rather than from the outside diameter).

Table 3. Bacteriophage and mammalian virus capsid dimensions based on structural models acquired from VIPERdb (TSRI, 2018). Structural files were not available for adenovirus 4, so adenovirus 5 (ADV 5) and 26 (ADV 26) were compared. Both adenovirus serotypes shared similar dimensions. The color scale indicates low (red) to high (green) capsid thickness.

		Bacteriophage				Mammalian Virus			
		fr	MS2	P22	ΦX174	FCV	ECV 12	ADV 5	ADV 26
Diameter (Å)	Outer	286	288	686	342	416	404	940	952
	Inner	210	210	534	192	236	212	632	630
	Avg.	276	276	662	336	410	398	906	914
Adjusted capsid thickness (Å)		33	33	64	72	87	93	137	142
Source File	PDB-ID	1FRS	2MS2	5UU5	2BPA	3M8L	2C8I	6CGV	5TX1
	Resolution (Å)	3.50	2.80	3.30	3.00	3.40	14.0	3.80	3.70
	Method [a]	XD	XD	EM	XD	XD	EM	XD	EM
	Primary Citation								

[a] XD: X-ray diffraction; EM: Electron microscopy.
[b] (Liljas et al., 1994).

[c] (Golmohammadi et al., 1993).
[d] (Hryc et al., 2017).
[e] (McKenna et al., 1992).
[f] (Ossiboff et al., 2010).
[g] (Pettigrew et al., 2006).
[h] (Kundhavai Natchiar et al., 2018).
[i] (Yu et al., 2017).

Capsid thickness increased from bacteriophages to the mammalian viruses:
MS2 ≈ fr < P22 < ΦX174 < FCV < ECV < ADV. The three bacteriophages with the thinnest capsids (fr, MS2, and P22) were also the most susceptible to inactivation due to EC. Though ΦX174 has only a slightly thicker capsid than P22 (~13%), electrostatic repulsion and aggregation can still explain the recalcitrance of ΦX174 to iron-based disinfection. On the other hand, the recalcitrance of FCV to iron-based disinfection may be due more to capsid structure, given its theoretically low pI but thicker (9 nm) capsid. The susceptibility of viruses to inactivation due to iron EC may therefore be a combination of electrostatic interactions and capsid structure. Capsid thickness would likely not play as large a role for uncharged disinfectants like hypochlorous acid that could permeate capsid pores more readily. Though thickness may be a rough indicator of capsid durability, a more detailed evaluation of capsid structure and function could provide greater insight into why mammalian viruses are more resistant to inactivation.

4. Conclusions

This is the first work to evaluate human virus mitigation and quantitatively assess the fate of viruses in iron EC. This research evaluated the effect of several water parameters on virus fate via EC; however, the complexity of natural water matrices merits further testing of virus mitigation in natural waters. Both apparent inactivation and physical removal were important mechanisms of mitigation via EC for three of the four bacteriophages evaluated: fr, MS2, and P22. However, ΦX174 and the three mammalian viruses (ADV, ECV, and FCV) showed the greatest mitigation due to physical removal and were less susceptible to ferrous inactivation. In representing virus mitigation, ΦX174 was the only bacteriophage surrogate resistant to ferrous inactivation, possibly due to electrostatic repulsion between ΦX174 and ferrous iron at pH 6 and/or shielding of ΦX174 virions in aggregates near neutral pH. Though electrostatic interactions between ferrous ions and virions likely explains at least some of the differences in inactivation efficacy between viruses, resistant viruses also had thicker capsids. The lack of experimental isoelectric point data for human viruses prevents a full analysis of this hypothesis. However, a detailed theoretical evaluation of capsid structure may provide additional insight where empirical methods are prohibitive.

Declaration of competing interest

The authors declare that they have no known competing financial interests or personal relationships that could have appeared to influence the work reported in this paper.

Acknowledgments

Funding for this project was provided by the National Science Foundation [grant number 1433003]. The GHR Foundation also provided partial support for the project, including purchase of the zetasizer and partial undergraduate research support for Mr. McDermid. Additional support for Mr. McDermid was provided by the Lafferty Family Foundation. Mr. Heffron's stipend was partially funded by a Marquette University Richard W. Jobling Research Assistantship and a fellowship from the Arthur J. Schmitt Foundation. The authors do not claim any competing interests.

Appendix A. Supplementary data

The following is the Supplementary data to this article: Download : **Download Word document (117KB)**

Multimedia component 1.

References

Adams, 1959, M.H. Adams, **Bacteriophages.** Interscience Publishers, New York (1959)

Amarasiri et al., 2017, M. Amarasiri, M. Kitajima, T.H. Nguyen, S. Okabe, D. Sano, **Bacteriophage removal efficiency as a validation and operational monitoring tool for virus reduction in wastewater reclamation: Review.** Water Res., 121 (2017), pp. 258-269. https://doi.org/10.1016/j.watres.2017.05.035

Armanious et al., 2015, A. Armanious, M. Aeppli, R. Jacak, D. Refardt, T. Sigstam, T. Kohn, M. Sander, **Viruses at solid-water interfaces: a systematic assessment of interactions driving adsorption.** Environ. Sci. Technol., 50 (2015), pp. 732-743. https://doi.org/10.1021/acs.est.5b04644

Averett et al., 1994, R. Averett, J. Leenheer, D. McKnight, K. Thorn, **Humic Substances in the Suwannee River, Georgia: Interactions, Properties and Proposed Structures.** US Government Printing Office, Washington, DC (1994)

Bae and Schwab, 2008, J. Bae, K.J. Schwab, **Evaluation of murine norovirus, feline calicivirus, poliovirus, and MS2 as surrogates for human norovirus in a model of viral persistence in surface water and groundwater.** Appl. Environ. Microbiol., 74 (2008), pp. 477-484. https://doi.org/10.1128/AEM.02095-06

Bagotsky, 2006, V.S. Bagotsky, **Fundamentals of Electrochemistry.** (second ed.), John Wiley & Sons, Inc, Hoboken, New Jersey (2006)

Beck et al., 2009, N.K. Beck, K. Callahan, S.P. Nappier, H. Kim, M.D. Sobsey, J.S. Meschke, **Development of a spot-titer culture assay for quantifying bacteria and viral indicators.** J. Rapid Methods Autom. Microbiol., 17 (2009), pp. 455-464. https://doi.org/10.1111/j.1745-4581.2009.00182.x

Cañizares et al., 2007, P. Cañizares, C. Jiménez, F. Martínez, C. Sáez, M.A. Rodrigo, **Study of the electrocoagulation process using aluminum and iron electrodes.** Ind. Eng. Chem. Res., 46 (2007), pp. 6189-6195. https://doi.org/10.1021/ie070059f

Cannon et al., 2006, J.L. Cannon, E. Papafragkou, G.W. Park, J. Osborne, L.-A. Jaykus, J. Vinjé, **Surrogates for the study of norovirus stability and inactivation in the environment: a comparison of murine norovirus and feline calicivirus.** J. Food Prot., 69 (2006), pp. 2761-2765. https://doi.org/10.4315/0362-028X-69.11.2761

Centers for Disease Control and Prevention, 2015, Centers for Disease Control and Prevention, **Surveillance reports for drinking water-associated disease & outbreaks.** [WWW Document]. URL. https://www.cdc.gov/healthywater/surveillance/drinking-surveillance-reports.html (2015) accessed 7.7.17

Centers for Disease Control and Prevention, 2012, Centers for Disease Control and Prevention, **Effect of chlorination on inactivating selected pathogens.** [WWW Document]. URL http://www.cdc.gov/safewater/effectiveness-on-pathogens.html (2012) accessed 1.1.15

Chen and Soucie, 1986, W.S. Chen, W.G. Soucie, **The ionic modification of the surface charge and isoelectric point of soy protein.** J. Am. Oil Chem. Soc., 63 (1986), pp. 1346-1350 https://doi.org/10.1007/BF02679599

Crittenden et al., 2012, J.C. Crittenden, R.R. Trussell, D.W. Hand, K.J. Howe, G. Tchobanoglous, **MWH's Water Treatment: Principles and Design.** (third ed.), John Wiley & Sons, Inc., Hoboken, New Jersey (2012)

Delaire et al., 2015, C. Delaire, C.M. Van Genuchten, K.L. Nelson, S.E. Amrose, A.J. Gadgil, **Escherichia coli attenuation by Fe electrocoagulation in synthetic Bengal groundwater: effect of pH and natural**

organic matter. Environ. Sci. Technol., 49 (2015), pp. 9945-9953. https://doi.org/10.1021/acs.est.5b01696

Dubrawski et al., 2015, K.L. Dubrawski, C.M. Van Genuchten, C. Delaire, S.E. Amrose, A.J. Gadgil, M. Mohseni, **Production and transformation of mixed-valent nanoparticles generated by Fe(0) electrocoagulation.** Environ. Sci. Technol., 49 (2015), pp. 2171-2179 https://doi.org/10.1021/es505059d

EDR Group, 2013, EDR Group, **Failure to Act: the Impact of Current Infrastructure Investment on America's Economic Future.** American Society of Civil Engineers (2013)

Fidalgo De Cortalezzi et al., 2014, M.M. Fidalgo De Cortalezzi, M.V. Gallardo, F. Yrazu, G.J. Gentile, O. Opezzo, R. Pizarro, H.R. Poma, V.B. Rajal, **Virus removal by iron oxide ceramic membranes.** J. Environ. Chem. Eng., 2 (2014), pp. 1831-1840. https://doi.org/10.1016/j.jece.2014.08.006

Gall et al., 2015, A.M. Gall, B.J. Mariñas, Y. Lu, J.L. Shisler, **Waterborne viruses: a barrier to safe drinking water.** PLoS Pathog., 11 (2015), pp. 1-7. https://doi.org/10.1371/journal.ppat.1004867

Gerba and Betancourt, 2017, C.P. Gerba, W.Q. Betancourt, **Viral aggregation: impact on virus behavior in the environment.** Environ. Sci. Technol., 51 (2017), pp. 7318-7325 https://doi.org/10.1021/acs.est.6b05835

Golmohammadi et al., 1993, R. Golmohammadi, K. Valegard, K. Fridborg, L. Liljas, **The refined structure of bacteriophage MS2 at 2.8 A resolution.** J. Mol. Biol., 234 (1993), pp. 620-639. https://doi.org/10.2210/PDB2MS2/PDB

Grabow, 2007, W.O.K. Grabow, **Overview of health-related water virology.** A. Bosch (Ed.), Human Viruses in Water, Elsevier, Amstersdam (2007), pp. 1-26

Grabow, 2001, W.O.K. Grabow, **Bacteriophages: update on application as models for viruses in water.** Water S.A., 27 (2001), pp. 251-268 https://doi.org/10.4314/wsa.v27i2.4999

Hall, 2012, A.J. Hall, **Noroviruses: the perfect human pathogens?** J. Infect. Dis., 205 (2012), pp. 1622-1624 https://doi.org/10.1093/infdis/jis251

Harif et al., 2012, T. Harif, M. Khai, A. Adin, **Electrocoagulation versus chemical coagulation: coagulation/flocculation mechanisms and resulting floc characteristics.** Water Res., 46 (2012), pp. 3177-3188. https://doi.org/10.1016/j.watres.2012.03.034

Heffron, 2019, J. Heffron, **Iron-enhanced Mitigation of Viruses in Drinking Water.** Marquette University (2019)

Heffron and Mayer, 2016, J. Heffron, B.K. Mayer, **Virus mitigation by coagulation: recent discoveries and future directions.** Environ. Sci. Water Res. Technol., 2 (2016), pp. 443-459 https://doi.org/10.1039/C6EW00060F

Heffron et al., 2019a, J. Heffron, B. McDermid, B.K. Mayer, **Bacteriophage inactivation as a function of ferrous iron oxidation.** Environ. Sci. Water Res. Technol., 5 (2019), pp. 1309-1317 https://doi.org/10.1039/C9EW00190E

Heffron et al., 2019b, J. Heffron, D.R. Ryan, B.K. Mayer, **Sequential electrocoagulation-electrooxidation for virus mitigation in drinking water.** Water Res., 160 (2019), pp. 435-444 https://doi.org/10.1016/j.watres.2019.05.078

Hryc et al., 2017, C.F. Hryc, D.H. Chen, P.V. Afonine, J. Jakana, Z. Wang, C. Haase-Pettingell, W. Jiang, P.D. Adams, J.A. King, M.F. Schmid, W. Chiu, **Accurate model annotation of a near-atomic resolution cryo-EM map.** Proc. Natl. Acad. Sci. U.S.A., 114 (2017), pp. 3103-3108 https://doi.org/10.2210/PDB5UU5/PDB

Huling and Pivetz, 2006, S.G. Huling, B.E. Pivetz, **In-situ Chemical Oxidation.** United States Environmental Protection Agency (2006)

Jeong et al., 2006, J. Jeong, J.Y. Kim, J. Yoon, **The role of reactive oxygen species in the electrochemical inactivation of microorganisms.** Environ. Sci. Technol., 40 (2006), pp. 6117-6122 https://doi.org/10.1021/es0604313

Kim et al., 2011, J.Y. Kim, C. Lee, D.C. Love, D.L. Sedlak, J. Yoon, K.L. Nelson, **Inactivation of MS2 coliphage by ferrous ion and zero-valent iron nanoparticles.** Environ. Sci. Technol., 45 (2011), pp. 6978-6984 https://doi.org/10.1021/es201345y

Kreißel et al., 2014, K. Kreißel, M. Bösl, M. Hügler, P. Lipp, M. Franzreb, B. Hambsch, **Inactivation of F-specific bacteriophages during flocculation with polyaluminum chloride - a mechanistic study.** Water Res., 51 (2014), pp. 144-151. https://doi.org/10.1016/j.watres.2013.12.026

Kundhavai Natchiar et al., 2018, S. Kundhavai Natchiar, S. Venkataraman, T.M. Mullen, G.R. Nemerow, V.S. Reddy, **Revised crystal structure of human adenovirus reveals the limits on protein IX quasi-equivalence and on analyzing large macromolecular complexes.** J. Mol. Biol., 430 (2018), pp. 4132-4141 https://doi.org/10.1016/j.jmb.2018.08.011

Lakshmanan and Clifford, 2009, D. Lakshmanan, D.A. Clifford, **Ferrous and ferric ion generation during iron electrocoagulation.** Environ. Sci. Technol., 43 (2009), pp. 3853-3859

Leenheer et al., 1995, J.A. Leenheer, R.L. Wershaw, M.M. Reddy, **Strong-acid, carboxyl-group structures in fulvic acid from the Suwannee River, Georgia. 1. Minor structures.** Environ. Sci. Technol., 29 (1995), pp. 393-398 https://doi.org/10.1021/es00002a015

Li et al., 2012, L. Li, C.M. van Genuchten, S.E.A. Addy, J. Yao, N. Gao, A.J. Gadgil, **Modeling As(III) oxidation and removal with iron electrocoagulation in groundwater.** Environ. Sci. Technol., 46 (2012), pp. 12038-12045 https://doi.org/10.1021/es302456b

Liljas et al., 1994, L. Liljas, K. Fridborg, K. Valegård, M. Bundule, P. Pumpens, **Crystal structure of bacteriophage fr capsids at 3.5 A resolution.** J. Mol. Biol., 244 (1994), pp. 279-290 https://doi.org/10.1006/jmbi.1994.1729

Maher et al., 2019, E.K. Maher, K.N. O'Malley, J. Heffron, J. Huo, B.K. Mayer, Y. Wang, P.J. McNamara, **Analysis of operational parameters, reactor kinetics, and floc characterization for the removal of estrogens via electrocoagulation.** Chemosphere, 220 (2019), pp. 1141-1149 https://doi.org/10.1016/j.chemosphere.2018.12.161

Matsui et al., 2003, Y. Matsui, T. Matsushita, S. Sakuma, T. Gojo, T. Mamiya, H. Suzuoki, T. Inoue, **Virus inactivation in aluminum and polyaluminum coagulation.** Environ. Sci. Technol., 37 (2003), pp. 5175-5180

Mayer et al., 2008, B.K. Mayer, H. Ryu, M. Abbaszadegan, **Treatability of U.S. Environmental Protection Agency contaminant candidate list viruses: removal of coxsackievirus and echovirus using enhanced coagulation.** Environ. Sci. Technol., 42 (2008), pp. 6890-6896 https://doi.org/10.1021/es801481s

Mayer et al., 2015, B.K. Mayer, Y. Yang, D.W. Gerrity, M. Abbaszadegan, **The impact of capsid proteins on virus removal and inactivation during water treatment processes.** Microbiol. Insights, 8 (2015), pp. 15-28 https://doi.org/10.4137/Mbi.s31441.TYPE

McKenna et al., 1992, R. McKenna, D. Xia, P. Willingmann, L.L. Ilag, S. Krishnaswamy, M.G. Rossmann, N.H. Olson, T.S. Baker, N. L. Incardona.,**Atomic structure of single-stranded DNA bacteriophage phi X174 and its functional implications.** Nature, 355 (1992), pp. 137-143 https://doi.org/10.2210/PDB2BPA/PDB

Mechenich and Andrews, 2004, C. Mechenich, E. Andrews, **Interpreting Drinking Water Test Results.** (2004) UW Extension G3558-4

Michen and Graule, 2010, B. Michen, T. Graule, **Isoelectric points of viruses.** J. Appl. Microbiol., 109 (2010), pp. 388-397 https://doi.org/10.1111/j.1365-2672.2010.04663.x

Ndjomgoue-Yossa et al., 2015, A.C. Ndjomgoue-Yossa, C.P. Nanseu-Njiki, I.M. Kengne, E. Ngameni, **Effect of electrode material and supporting electrolyte on the treatment of water containing Escherichia coli by electrocoagulation.** Int. J. Environ. Sci. Technol., 12 (2015), pp. 2103-2110 https://doi.org/10.1007/s13762-014-0609-9

Ossiboff et al., 2010, R.J. Ossiboff, Y. Zhou, P.J. Lightfoot, B.V. Prasad, J.S. Parker, **Conformational changes in the capsid of a calicivirus upon interaction with its functional receptor.** J. Virol., 84 (2010), pp. 5550-5564 https://doi.org/10.2210/PDB3M8L/PDB

Pettigrew et al., 2006, D.M. Pettigrew, D.T. Williams, D. Kerrigan, D.J. Evans, S.M. Lea, D. Bhella, **Structural and functional insights into the interaction of echoviruses and decay-accelerating factor.** J. Biol. Chem., 281 (2006), p. 5169 https://doi.org/10.2210/PDB2C8I/PDB

Powder Technology Inc., 2016, Powder Technology Inc., **Safety Data Sheet: Arizona Test Dust** (2016)

Prasad et al., 1994, B.V.V. Prasad, D.O. Matson, A.W. Smith, **Three-dimensional structure of calicivirus.** J. Mol. Biol., 240 (1994), pp. 256-264, 10.1006/jmbi.1994.1439 pii: S0022-2836(84)71439-2

R Core Team, 2014, R Core Team, **R: A Language and Environment for Statistical Computing.** (2014)

Reed and Muench, 1938, L.J. Reed, H. Muench, **A simple method of estimating fifty per cent endpoints.** Am. J. Hyg., 27 (1938), pp. 493-497 https://doi.org/10.1093/OXFORDJOURNALS.AJE.A118408

Samandoulgou et al., 2015, I. Samandoulgou, I. Fliss, J. Jean, **Zeta potential and aggregation of virus-like particle of human norovirus and feline calicivirus under different physicochemical conditions.** Food Environ. Virol., 7 (2015), pp. 249-260 https://doi.org/10.1007/s12560-015-9198-0

Shen et al., 2008, C. Shen, M.S. Phanikumar, T.-T. Fong, I. Aslam, S.P. Mcelmurry, S.L. Molloy, J.B. Rose, **Evaluating bacteriophage P22 as a tracer in a complex surface water system: the Grand River, Michigan.** Environ. Sci. Technol., 42 (2008), pp. 2426-2431 https://doi.org/10.1021/es702317t

Shirasaki et al., 2016, N. Shirasaki, T. Matsushita, Y. Matsui, T. Marubayashi, **Effect of aluminum hydrolyte species on human enterovirus removal from water during the coagulation process.** Chem. Eng. J., 284 (2016), pp. 786-793 https://doi.org/10.1016/j.cej.2015.09.045

Shirasaki et al., 2009, N. Shirasaki, T. Matsushita, Y. Matsui, T. Urasaki, K. Ohno, **Comparison of behaviors of two surrogates for pathogenic waterborne viruses, bacteriophages Qβ and MS2, during the aluminum coagulation process.** Water Res., 43 (2009), pp. 605-612 https://doi.org/10.1016/j.watres.2008.11.002

Song et al., 2017, Y. Song, G. Jiang, Y. Chen, P. Zhao, Y. Tian, **Effects of chloride ions on corrosion of ductile iron and carbon steel in soil environments.** Sci. Rep., 7 (2017), pp. 1-13 https://doi.org/10.1038/s41598-017-07245-1

Springthorpe and Sattar, 2007, S. Springthorpe, S.A. Sattar, **Virus removal during drinking water treatment.** Bosch (Ed.), Human Viruses in Water, Elsevier, Amstersdam (2007), pp. 109-126

Sun et al., 2013, L. Sun, L.N. Young, X. Zhang, S.P. Boudko, A. Fokine, E. Zbornik, A.P. Roznowski, I.J. Molineux, M.G. Ross mann, B.A. Fane, **Icosahedral bacteriophage ΦX174 forms a tail for DNA transport during infection.** Nature, 505 (2013), pp. 432-435 https://doi.org/10.1038/nature12816

Tanneru and Chellam, 2013, C.T. Tanneru, S. Chellam, **Sweep flocculation and adsorption of viruses on aluminum flocs during electrochemical treatment prior to surface water microfiltration.** Environ. Sci. Technol., 47 (2013), pp. 4612-4618

Tanneru and Chellam, 2012, C.T. Tanneru, S. Chellam, **Mechanisms of virus control during iron electrocoagulation--microfiltration of surface water.** Water Res., 46 (2012), pp. 2111-2120 https://doi.org/10.1016/j.watres.2012.01.032

Tanneru et al., 2014, C.T. Tanneru, N. Jothikumar, V.R. Hill, S. Chellam, **Relative insignificance of virus inactivation during aluminum electrocoagulation of saline waters.** Environ. Sci. Technol., 48 (2014), pp. 14590-14598 https://doi.org/10.1021/es504381f

TSRI, 2018, TSRI, **ViperDB.** [WWW document]. URL http://viperdb.scripps.edu/ (2018) accessed 11.30.18

US Environmental Protection Agency, 2016, US Environmental Protection Agency, **Microbial contaminants - CCL 4.** [WWW document]. URL https://www.epa.gov/ccl/microbial-contaminants-ccl-4 (2016)

Wilhelmsen, 1987, W. Wilhelmsen, **Passive behaviour of titanium in alkaline.** Electrochim. Acta, 32 (1987), pp. 85-89

World Health Organization, 1996, World Health Organization, **Guidelines for Drinking-Water Quality: Health Criteria and Other Supporting Information.** (second ed.), World Health Organization, Geneva (1996)

Xagoraraki et al., 2014, I. Xagoraraki, Z. Yin, Z. Svambayev, **Fate of viruses in water systems.** J. Environ. Eng., 140 (2014) 040140201–18 https://doi.org/10.1061/(ASCE)EE.1943-7870.0000827

Yu et al., 2017, X. Yu, D. Veesler, M.G. Campbell, M.E. Barry, F.J. Asturias, M.A. Barry, V.S. Reddy, **Cryo-EM structure of human adenovirus D26 reveals the conservation of structural organization among human adenoviruses.** Sci. Adv., 3 (2017) e1602670–e1602670 https://doi.org/10.2210/PDB5TX1/PDB

Zhu et al., 2005a, B. Zhu, D.A. Clifford, S. Chellam, **Virus removal by iron coagulation-microfiltration.** Water Res., 39 (2005), pp. 5153-5161 https://doi.org/10.1016/j.watres.2005.09.035

Zhu et al., 2005b, B. Zhu, D.A. Clifford, S. Chellam, **Comparison of electrocoagulation and chemical coagulation pretreatment for enhanced virus removal using microfiltration membranes.** Water Res., 39 (2005), pp. 3098-3108 https://doi.org/10.1016/j.watres.2005.05.020